

# The Pivotal Information Criterion

Sylvain Sardy  
Maxime van Cutsem  
*Department of Mathematics*  
*University of Geneva*

SYLVAIN.SARDY@UNIGE.CH  
MAXIME.VANCUTSEM@UNIGE.CH

Sara van de Geer  
*ETHZ*

VSARA@ETHZ.CH

## Abstract

The Bayesian and Akaike information criteria aim at finding a good balance between under- and over-fitting. They are extensively used every day by practitioners. Yet we contend they suffer from at least two afflictions: their penalty parameter  $\lambda = \log n$  and  $\lambda = 2$  are too small, leading to many false discoveries, and their inherent (best subset) discrete optimization is infeasible in high dimension. We alleviate these issues with the pivotal information criterion: PIC is defined as a continuous optimization problem, and the PIC penalty parameter  $\lambda$  is selected at the detection boundary (under pure noise). PIC's choice of  $\lambda$  is the quantile of a statistic that we prove to be (asymptotically) pivotal, provided the loss function is appropriately transformed. As a result, simulations show a phase transition in the probability of exact support recovery with PIC, a phenomenon studied with no noise in compressed sensing. Applied on real data, for similar predictive performances, PIC selects the least complex model among state-of-the-art learners.

**Keywords:** Compressed sensing, model selection, phase transition, pivotal statistic, sparsity.

## 1 Introduction

As computing power and data storage capacity continue to increase, along with advances in optimization algorithms, researchers and practitioners allow themselves to consider highly flexible models with growing numbers of parameters. Such flexibility may come at the expense of interpretability, parsimony, and sometimes scientific insight, as predictive performance alone becomes the primary objective.

We are focusing on model frugality and interpretability through the use of an information criterion to search for a parsimonious model and to control the overfitting without relying on a validation set. To illustrate our objective, we consider the linear regression model

$$\mathbf{y} = \beta_0 \mathbf{1} + X\boldsymbol{\beta} + \boldsymbol{\epsilon}, \tag{1}$$

where  $X$  is an  $n \times p$  matrix,  $\boldsymbol{\beta} \in \mathbb{R}^p$  is the parameter vector of interest,  $\boldsymbol{\epsilon}$  are errors with variance  $\sigma^2$ , and the intercept  $\beta_0$  and  $\sigma^2$  are nuisance parameters. A well-studied setting is the high-dimensional canonical linear model when  $y_i = \beta_i + \epsilon_i$  for  $i = 1, \dots, n$ , with  $n = p$  (i.e.,  $X = I_n$ ) and Gaussian errors. This simplified model has provided important insights into parameter estimation. In particular, the James-Stein estimator, a regularized maxi-

mum likelihood estimator (James and Stein, 1961), showed that the maximum likelihood estimator  $\hat{\boldsymbol{\beta}}^{\text{MLE}} = \mathbf{y}$  is inadmissible when  $p > 2$ .

As the number of predictors grows, assuming  $\boldsymbol{\beta}$  to be sparse became natural and amounts to assuming only a small portion of inputs are believed to contain predictive information. The parameter vector  $\boldsymbol{\beta}$  is called sparse if

$$\mathcal{S} = \{j \in \{1, \dots, p\} : \beta_j \neq 0\} \quad (2)$$

has a small cardinality  $s := |\mathcal{S}|$ . For a linear model (1),  $\mathcal{S}$  identifies the inputs with predictive information, often referred to as "needles in a haystack". The resulting paradigm centers on detecting these needles, a task closely related to testing.

### 1.1 Detection boundary and phase transition

Within this sparse paradigm, Donoho and Johnstone (1994) in regression, and Ingster (1997) and Donoho and Jin (2004) in hypothesis testing, showed the existence of a *detection boundary* below which signal recovery is hopeless. Specifically, if the nonzero entries of  $\boldsymbol{\beta}$  are below  $\sigma\sqrt{2r \log n}$ , where  $r \in (0, 1)$  is a sparsity index, then the nonzero entries are undetectable, otherwise detection becomes possible. This observation suggests thresholding observations whose magnitude falls below  $\varphi = \sigma\sqrt{2r \log n}$ , since attempting to estimate such components otherwise leads to excessive false discoveries. In particular, in wavelet smoothing, setting the threshold to  $\varphi = \sigma\sqrt{2 \log n}$  led to minimax properties (Donoho and Johnstone, 1994; Donoho et al., 1995). Ingster et al. (2010) extended the results to high-dimensional regression when the matrix  $X$  is no longer the identity.

Observed in the testing framework, a phase transition at the detection boundary has also been observed in compressed sensing (Donoho, 2006; Candès and Romberg, 2007), corresponding to the noiseless linear model  $\mathbf{y} = X\boldsymbol{\beta}$ , where  $X$  is  $n \times p$  with  $p > n$  and  $\boldsymbol{\beta}$  is assumed  $s$ -sparse. For small sparsity levels and moderate dimensions, by using the  $\ell_1$ -minimization estimator  $\min_{\boldsymbol{\beta} \in \mathbb{R}^p} \|\boldsymbol{\beta}\|_1$  subject to  $\mathbf{y} = X\boldsymbol{\beta}$ , exact recovery occurs with probability one, but this probability sharply drops to zero as  $s/p$  or  $p/n$  increases beyond critical thresholds. LASSO (Tibshirani, 1996) extends this approach to noisy settings by solving  $\min_{\boldsymbol{\beta} \in \mathbb{R}^p} \|\mathbf{y} - X\boldsymbol{\beta}\|_2^2 + \lambda \|\boldsymbol{\beta}\|_1$ , for some regularization parameter  $\lambda > 0$  chosen to optimize the prediction risk (e.g., via cross-validation), although this choice often fails to recover the true support  $\mathcal{S}$  (Su et al., 2015).

### 1.2 Information criteria

The learner we consider here aims at good estimation of  $\boldsymbol{\beta}$ , in particular detection of its nonzero entries, and is defined as a minimizer of an information criterion (IC). For a model parametrized by  $\boldsymbol{\beta} \in \mathbb{R}^p$ , and an intercept  $\beta_0 \in \mathbb{R}$  and (possibly) a nuisance parameter  $\sigma$ , an IC takes the form

$$\text{IC} = L(\boldsymbol{\beta}, \beta_0, \sigma; \mathcal{D}) + \lambda C(\boldsymbol{\beta}), \quad (3)$$

where  $\mathcal{D} = (X, \mathbf{y}) \in \mathbb{R}^{n \times (p+1)}$  denotes the data,  $L$  measures goodness of fit, and  $C$  quantifies model complexity. The tuning parameter  $\lambda > 0$  is fixed a priori (i.e., without validation data or cross-validation) and looks for an ideal compromise between the beliefs in  $L$  and  $C$  to select a model of appropriate dimension, thereby controlling under- and overfitting.

Among information criteria, BIC (Schwarz, 1978) is arguably the most widely used. It employs twice the negative log-likelihood for  $L$  and the discrete complexity measure

$$C(\boldsymbol{\beta}) = \|\boldsymbol{\beta}\|_0 = \#\{\beta_j \neq 0, j = 1, \dots, p\} =: s \in \{0, 1, \dots, p\} \quad (4)$$

which counts the number  $s$  of active parameters. For BIC, the preset value is  $\lambda = \log n$ , whereas AIC adopts  $\lambda = 2$  (Akaike, 1998). Minimizing either criterion yields sparse estimators  $\hat{\boldsymbol{\beta}}$ , in which some entries are exactly zero, facilitating interpretability by identifying influential inputs. The choice of  $\lambda$  is crucial: smaller values tend to produce overly complex models that may overfit and include many false positives, while larger values favor excessive sparsity.

A natural desideratum while minimizing the IC (3) is recovery of the truly relevant inputs of the linear model (1), that is, matching  $\hat{\mathcal{S}} = \{j \in \{1, \dots, p\} : \hat{\beta}_j \neq 0\}$  with  $\mathcal{S}$  in (2). This motivates studying the probability of exact support recovery,

$$\text{PESR} = \mathbb{P}(\hat{\mathcal{S}} = \mathcal{S}), \quad (5)$$

and its phase transition behavior as a function of  $s = |\mathcal{S}|$ , analogous to compressed sensing. This stringent property is not achieved by classical criteria such as BIC or AIC, even in ideal conditions such as independence of the inputs and high signal-to-noise ratio. Although dependence among columns of  $X$  further complicates recovery, the independent-design setting provides an ideal benchmark for comparing sparse learners.

We use the Gaussian linear regression setting to illustrate limitations of BIC, to which we discuss our proposed remedy in Section 2. Assuming Gaussian errors with variance  $\sigma^2$ ,

$$\text{BIC} = \frac{1}{\sigma^2} \text{RSS}_s + \lambda s + n \log \sigma^2 \quad \text{with} \quad \lambda = \log n,$$

where the best size- $s$  residual sum of squares are

$$\text{RSS}_s := \min_{\beta_0 \in \mathbb{R}, \boldsymbol{\beta} \in \Omega_s} \|\mathbf{y} - \beta_0 \mathbf{1}_n - X\boldsymbol{\beta}\|_2^2 \quad \text{with} \quad \Omega_s = \{\boldsymbol{\beta} \in \mathbb{R}^p : \|\boldsymbol{\beta}\|_0 = s\}. \quad (6)$$

Minimizing over  $s \in \{0, 1, \dots, \min(n, p)\}$  yields a selected sparsity level  $\hat{s}$ . AIC replaces  $\lambda = \log n$  with  $\lambda = 2$ , leading to a less sparse model when  $n > \exp(2)$ . Regardless of whether one uses BIC, AIC, or some high-dimensional extensions such as Chen and Chen (2008, EBIC) and Fan and Tang (2013, GIC), these criteria depend on the nuisance parameter  $\sigma^2$ , whose estimation becomes challenging in high-dimensional settings ( $p > n$ ); see, e.g., Fan et al. (2012). Using the maximum likelihood estimate  $\hat{\sigma}^{2, \text{MLE}} = \text{RSS}_s/n$  yields the profile criterion (up to constants)

$$\text{BIC} = \log \frac{\text{RSS}_s}{n} + s \frac{\log n}{n}.$$

Optimizing over  $s$  is NP-hard since it requires searching over all predictor subsets. In practice, one relies on approximations such as greedy forward selection or the primal-dual active set (PDAS) method of Ito and Kunisch (2014).

The discrete optimization behind BIC is certainly cumbersome, but the main reason why BIC fails to retrieve  $\mathcal{S}$  stems from the choice  $\lambda = \log n$ . Schwarz (1978) derived this term via a large-sample approximation to the Bayes factor, whose primary goal is model

comparison rather than exact support recovery. Consequently, despite its widespread use, BIC is poorly suited for recovering  $\mathcal{S}$ , which in practice leads to suboptimal generalization and interpretability. Section 3 illustrates this point empirically by comparing BIC to our proposed information criterion.

### 1.3 Our proposal and paper organization

We aim at constructing a learner that exhibits a phase transition analogous to compressed sensing, but in the presence of noise. Specifically, when  $s/p$  or  $p/n$  are small, the learner should recover  $\mathcal{S}$  with high probability, while this probability eventually drops to zero as these ratios increase and the non-zero components of  $\beta$  become undetectable. We calibrate the learner such that, when  $s = 0$ , the probability of retrieving  $\mathcal{S} = \emptyset$  is set to  $1 - \alpha$ , for some prescribed small  $\alpha$ . Starting from a high probability when  $s = 0$  mimics the unit probability property of compressed sensing for small complexity index  $s$ ; this provides a favorable initialization. Our *pivotal information criterion* (PIC) achieves the desirable property with a pre-specified value of  $\lambda$  set at the detection boundary. The key novelty is the introduction of two transformation functions  $\phi$  and  $g$ , which render the choice of the regularization parameter  $\lambda$  pivotal (i.e., independent of unknown parameters). PIC provides a general framework that applies broadly across multiple distributions and accommodates continuous complexity penalties  $C(\beta)$ .

This paper is organized as follows. Section 2 introduces the pivotal information criterion: Section 2.1 gives its formal definition, Section 2.2 introduces the concept of a zero-thresholding function, Section 2.3 explains how to make the information criterion (asymptotic) pivotal, Section 2.4 discusses practical implementations and Section 2.5 derives the appropriate parameter  $\lambda$  for BIC. Section 3 quantifies the validity of the theory and the empirical performance of PIC: Section 3.1 illustrates graphically the pivotality of PIC, Section 3.2 performs Monte-Carlo simulations to observe the phase transitions in different settings, and Section 3.3 applies various methods to six datasets to investigate the trade-off between generalization and complexity. Section 4 finishes with some general comments.

## 2 The pivotal information criterion

Many sparse learners such as Basis Pursuit (Chen et al., 1999), LASSO, or Elastic Net (Zou and Hastie, 2005) rely on continuous penalties, whereas AIC and BIC use a discrete complexity measure. However, what primarily distinguishes an information criterion (3) from a sparse learner is that the regularization parameter  $\lambda$  is *pre-set*. Indeed, while learners select  $\lambda$  from the data (e.g., via cross-validation), ICs rely on a closed-form model-based calibration (e.g.,  $\lambda = \log n$  for BIC). Two notable learners also use pre-set regularization parameters: wavelshrink chooses  $\lambda = \sigma\sqrt{2\log n}$  (Donoho and Johnstone, 1994; Donoho et al., 1995) and square-root LASSO (Belloni et al., 2011) chooses  $\lambda$  as a quantile of a pivotal statistic. The former depends on the nuisance parameter  $\sigma$  and is therefore not pivotal, whereas the latter is.

## 2.1 Definition

The pivotal information criterion (PIC) we propose can be seen as a generalization of square-root LASSO beyond Gaussianity and uses a pre-set value for the regularization parameter. Our key principle is to choose  $\lambda$  at the detection boundary, formalized below.

**Definition 1** *Let  $\hat{\beta}_\lambda$  be a sparse learner indexed by  $\lambda$ , and let  $\alpha$  be a prescribed small probability. Under  $H_0 : \beta = \mathbf{0}$ , the value  $\lambda_\alpha$  such that  $\mathbb{P}_{H_0}(\hat{\beta}_{\lambda_\alpha} = \mathbf{0}) = 1 - \alpha$  is the  $\alpha$ -level detection boundary. If  $\lambda_\alpha$  does not depend on nuisance parameters, then we call  $\lambda_\alpha^{\text{PDB}}$  the pivotal detection boundary.*

Choosing  $\lambda < \lambda_\alpha$  leads to high false discovery rate, whereas  $\lambda > \lambda_\alpha$  unnecessarily compromises the chance of finding the needles. Waveshrink satisfies this property asymptotically as  $\alpha \rightarrow 0$  (Donoho and Johnstone, 1994, equation (31)).

Since discrete penalties lead to NP-hard problems, PIC instead relies on a class of continuous complexity measures  $\mathcal{C}_{\ell_1}$  to facilitate optimization.

**Definition 2** *Let  $\rho : \mathbb{R} \rightarrow [0, \infty)$  be even and nondecreasing on  $\mathbb{R}^+$ . For  $\beta \in \mathbb{R}^p$ , define  $C(\beta) = \sum_{i=1}^p \rho(\beta_i)$ . We say that  $C \in \mathcal{C}_{\ell_1}$  is a first-order  $\ell_1$ -equivalent complexity penalty if  $\lim_{\epsilon \rightarrow 0^+} \frac{C(\epsilon\beta)}{\epsilon} = \|\beta\|_1$ .*

This class of measures models complexity through the magnitude of the coefficients. It includes convex penalties (e.g.,  $\ell_1$ ) and nonconvex ones such as SCAD (Fan and Li, 2001) and MCP (Zhang, 2010) penalties. Although they may differ away from zero, all behave like the  $\ell_1$  norm to first order near the origin, thereby promoting sparsity. If one still desires to use BIC's discrete complexity measure (4), Section 2.5 shows how our method still applies to find a good  $\lambda$  for BIC.

The pivotal information criterion can now be defined.

**Definition 3** *Given data  $\mathcal{D}$ , a base loss  $l_n(\theta, \sigma; \mathcal{D}) = \sum_{i=1}^n l(\theta_i, \sigma; \mathcal{D}_i)/n$ , a complexity measure  $C \in \mathcal{C}_{\ell_1}$ , parameters  $\beta \in \mathbb{R}^p$ , nuisance parameters  $\beta_0 \in \mathbb{R}$  and  $\sigma$ , and  $\alpha \in (0, 1)$ , the Pivotal Information Criterion is*

$$\text{PIC} = \phi(l_n(\theta, \sigma; \mathcal{D})) + \lambda_\alpha^{\text{PDB}} C(\beta) \quad \text{with} \quad \theta = g(\beta_0 \mathbf{1} + X\beta), \quad (7)$$

where the pre-set value of the complexity penalty  $\lambda_\alpha^{\text{PDB}}$  of Definition 1 is made pivotal thanks to the univariate functions  $\phi$  and  $g$  (applied componentwise), if they exist.

By construction, PIC takes the IC form defined in (3) with composite loss  $L = (\phi \circ l_n \circ g)$ . Finding the functions  $(\phi, g)$  is linked to the existence of a zero-thresholding function, which we discuss in Section 2.2. Section 2.3 derives  $(\phi, g)$  for the location-scale and the one-parameter exponential families, and Section 2.4 shows how to implement  $\lambda_\alpha^{\text{PDB}}$  in practice. Section 2.5 derives  $\lambda_\alpha^{\text{PDB}}$  for BIC's nostalgics.

## 2.2 Zero-thresholding function

Consider a sparse learner  $\hat{\beta}_\lambda$  defined as the minimizer of the IC defined in (3) with  $C \in \mathcal{C}_{\ell_1}$ . Under regularity conditions, there exists a finite value  $\lambda_0 > 0$  such that  $\hat{\beta}_\lambda = \mathbf{0}$  is a local minimizer of (3) if and only if  $\lambda \geq \lambda_0$ . When the cost function (3) is convex, this local minimum is also global. The smallest such  $\lambda$  admits a simple characterization, called zero-thresholding function.

**Theorem 4 (Zero-thresholding function)** *Let  $\hat{\beta}_\lambda$  minimize (3) and denote  $\boldsymbol{\tau} = (\beta_0, \sigma)$  the nuisance parameters. Assume  $L$  is twice differentiable at  $(\mathbf{0}, \hat{\boldsymbol{\tau}})$ , where  $\hat{\boldsymbol{\tau}}$  satisfies  $\nabla_{\boldsymbol{\tau}} L(\mathbf{0}, \hat{\boldsymbol{\tau}}; \mathcal{D}) = \mathbf{0}$  and the Hessian  $H_{\boldsymbol{\tau}}^L(\mathbf{0}, \hat{\boldsymbol{\tau}}) \succ 0$ . Then the zero-thresholding function*

$$\lambda_0(L, \mathcal{D}) = \|\nabla_{\beta} L(\mathbf{0}, \hat{\boldsymbol{\tau}}; \mathcal{D})\|_{\infty} \quad (8)$$

*satisfies that  $(\mathbf{0}, \hat{\boldsymbol{\tau}})$  is a local minimizer of (3) if and only if  $\lambda \geq \lambda_0(L, \mathcal{D})$ .*

For example, the zero-thresholding function of LASSO is  $\lambda_0(L, \mathcal{D}) = \|X^T(\mathbf{y} - \bar{y}\mathbf{1})\|_{\infty}$  and that of square-root LASSO is  $\lambda_0(L, \mathcal{D}) = \|X^T(\mathbf{y} - \bar{y}\mathbf{1})\|_{\infty} / \|\mathbf{y} - \bar{y}\mathbf{1}\|_2$ . Giacobino et al. (2017) derive the zero-thresholding functions of well-known sparse learners.

The  $\alpha$ -level detection boundary of Definition 1 can now be defined for sparse learners defined as solution to an IC of the form (3).

**Proposition 5** *Consider the learner  $\hat{\beta}_\lambda$  of Theorem 4. Let  $\mathbf{Y}_0 \sim p_{\boldsymbol{\tau}}$  denote observations generated under the pure-noise model ( $\boldsymbol{\beta} = \mathbf{0}$  and  $\boldsymbol{\tau} = (\beta_0, \sigma)$ ). Define the random variable*

$$\Lambda = \lambda_0(L, (X, \mathbf{Y}_0))$$

*and let  $F_{\Lambda}$  denote its cumulative distribution function. Setting  $\lambda_{\alpha} = F_{\Lambda}^{-1}(1 - \alpha)$  yields  $\mathbb{P}\left(\{\hat{\beta}_{\lambda_{\alpha}} = \mathbf{0} \text{ is a local minimizer of (3)}\}\right) = 1 - \alpha$ .*

This is a direct consequence of Theorem 4.

The value  $\lambda_{\alpha}$  cannot be computed directly in practice because the statistic  $\Lambda$  may depend on the unknown nuisance parameters  $\boldsymbol{\tau} = (\beta_0, \sigma)$  that generated the data at hand. Moreover, real datasets rarely arise from the pure-noise model, so reliable estimation of  $\beta_0$  or  $\sigma$ , especially in high-dimensional settings, is therefore challenging, resulting in poor calibration of  $\lambda_{\alpha}$ . By rather employing PIC (7), whose transformed loss is  $L(\boldsymbol{\beta}, \beta_0, \sigma; \mathcal{D}) = (\phi \circ l_n)(g(\beta_0\mathbf{1} + X\boldsymbol{\beta}), \sigma; \mathcal{D})$ , the law of  $\Lambda$  can be made asymptotically pivotal through a zero-thresholding function involving  $\phi'$  and  $g'$ .

**Proposition 6** *Consider PIC (7), where  $\phi$  and  $g$  are strictly increasing differentiable functions. Define the scalar-restricted loss  $\tilde{l}_n(\theta, \sigma; \mathcal{D}) := l_n(\theta\mathbf{1}_n, \sigma; \mathcal{D})$ . Assume that under the null model  $\boldsymbol{\beta} = \mathbf{0}$  there exists  $\hat{\boldsymbol{\tau}} = (\hat{\beta}_0, \hat{\sigma})$  such that  $g(\hat{\beta}_0) = \hat{\theta}^{\text{MLE}}$  and  $\hat{\sigma} = \hat{\sigma}^{\text{MLE}}$ , and that the scalar-restricted Hessian satisfies  $\nabla_{(\theta, \sigma)}^2 \tilde{l}_n(\hat{\theta}^{\text{MLE}}, \hat{\sigma}; \mathcal{D}) \succ 0$ . Then the zero-thresholding function of PIC is*

$$\lambda_0(\phi \circ l_n \circ g, \mathcal{D}) = \phi' \left( \tilde{l}_n \left( \hat{\theta}^{\text{MLE}}, \hat{\sigma}; \mathcal{D} \right) \right) \cdot g' \left( g^{-1}(\hat{\theta}^{\text{MLE}}) \right) \cdot \left\| X^T \nabla_{\boldsymbol{\theta}} l_n \left( \hat{\theta}^{\text{MLE}} \mathbf{1}, \hat{\sigma}; \mathcal{D} \right) \right\|_{\infty}.$$

Theorem 4 requires  $H_{\boldsymbol{\tau}}^L(\mathbf{0}, \hat{\boldsymbol{\tau}}) \succ 0$  for the composite loss  $L = \phi \circ l_n \circ g$ . A direct second-order differentiation with respect to  $(\beta_0, \sigma)$ , together with the score equations eliminating first-order terms and the separable character of  $l_n$ , shows that this condition reduces to positive definiteness of the Hessian of  $\tilde{l}_n$  at  $(\hat{\theta}^{\text{MLE}}, \hat{\sigma})$ . The expression for  $\lambda_0$  then follows from the chain rule. Notably,  $\lambda_0$  does not depend on the specific penalty  $C$ , provided  $C \in \mathcal{C}_{\ell_1}$ .

### 2.3 Finding $(\phi, g)$

The transformations  $(\phi, g)$  play a central role in rendering  $\Lambda$  pivotal (Proposition 5), enabling calibration of  $\lambda$  at the detection boundary without accurate estimation of nuisance parameters. The function  $g$  transforms the input of the loss  $l_n$  and is reminiscent of the link function of generalized linear models (Nelder and Wedderburn, 1972) and of variance stabilizing transformations (Bartlett, 1947). The function  $\phi$  rather transforms the output of the loss. It is important to observe that  $\phi \circ l_n \circ g$  employed by PIC is just a composite loss function, but by no means it models the mechanism that generated the data through functions  $g$  and  $\phi$ . Take the Poisson law for instance, the data can be generated from a linear model with the exponential canonical link, yet PIC’s composite loss may employ a function  $g \neq \exp$  to make the choice of  $\lambda$  pivotal. Similarly, it is common practice to fit a linear model with the  $\ell_2$  loss even when the data are Poisson.

To find a pivotal pair  $(\phi, g)$ , we consider loss functions  $l_n$  of two classes of distributions: the location-scale and one-parameter exponential families. We let  $\mathcal{D} = (X, \mathbf{y})$  be the data, where  $\mathbf{y}$  are realizations from  $Y_1, \dots, Y_n$ .

Employing the exponential transformation for  $\phi$ , the following theorem states the finite sample pivotality of PIC’s penalty for the location scale family.

**Theorem 7 (Location–scale family)** *Assume  $f$  is a fixed baseline density such that, conditionally on  $\mathbf{x}_i$ ,*

$$f_{Y_i}(y_i \mid \mathbf{x}_i; \theta_i, \sigma) = \frac{1}{\sigma} f\left(\frac{y_i - \theta_i}{\sigma}\right), \quad f(\cdot) > 0 \text{ on } \mathbb{R}, \quad \sigma > 0,$$

where  $\theta_i = g(\beta_0 + \mathbf{x}_i^T \boldsymbol{\beta})$ . Let  $l_n(\boldsymbol{\theta}, \sigma; \mathcal{D})$  be the average negative log-likelihood satisfying Proposition 6. Then PIC is finite-sample pivotal for  $(\phi, g) = (\exp, \text{id})$ .

We refer to the resulting estimator as *exponential LASSO*. The exponential transformation implies that exponential LASSO solves

$$\min_{\boldsymbol{\beta}, \beta_0, \sigma} (1/f_{\mathbf{Y}}(\mathbf{y}; \boldsymbol{\beta}, \beta_0, \sigma))^{1/n} + \lambda \|\boldsymbol{\beta}\|_1.$$

Profiling over  $\sigma$  yields  $l_n(\boldsymbol{\theta}, \sigma; \mathcal{D}) \propto \frac{1}{n} (\sum_i |y_i - \theta_i|^r)^{1/r}$ , recovering square-root LASSO when  $r = 2$ . This means that the  $r$ th root is the transformation that makes the  $r$ -th loss pivotal, as stated in the following property.

**Property 1** *For the Subbotin family (including the Gaussian case  $r = 2$ ) with density  $f_{\mathbf{Y}}(y; \mu, \sigma) \propto \sigma^{-1} \exp(-|y - \mu|/\sigma^r)$ , the pivotal transformation for the loss  $l_n(\boldsymbol{\theta}, \sigma; \mathcal{D}) = \frac{1}{n} \sum_i |y_i - \theta_i|^r$  is  $(\phi, g) = (u^{1/r}, \text{id})$ .*

Other location–scale distributions than Subbotin include Gumbel and logistic laws. Asymptotic convergence properties of PIC for this family are studied in van de Geer et al. (2025), and Section 3 illustrates the resulting phase-transition behavior empirically.

We now consider the one-parameter exponential family for which, conditionally on  $\mathbf{x}_i$ ,  $\log f_{Y_i}(y_i \mid \mathbf{x}_i; \theta_i) = \theta_i T(y_i) - d(\theta_i) + b(y_i)$ , where the canonical parameter satisfies  $\theta_i = g(\beta_0 + \mathbf{x}_i^T \boldsymbol{\beta})$  with  $g = \text{id}$ . We develop two approaches. The first one, described in Theorem

8, uses the classical negative log-likelihood as loss function  $l_n$  and searches for a pivotal link function  $g$ . The second one, described in Theorem 9, introduces a new class of losses yielding a weighted gradient allowing pivotality, yet keeping  $g = \text{id}$ .

**Condition 1** *The vectors of variables  $\mathbf{x}_1, \dots, \mathbf{x}_n \in \mathbb{R}^p$  in  $X$  are fixed, uniformly bounded  $|x_{ij}| \leq B_n$ , and standardized so that  $\sum_{i=1}^n \mathbf{x}_i = \mathbf{0}$  and  $\sum_{i=1}^n x_{ij}^2 = n$  for  $j = 1, \dots, p$ .*

**Condition 2** *The number of variables  $p$  is allowed to tend to infinity such that  $B_n^4(\log(pn))^7 = O(n^{1-c})$  for some  $c > 0$ .*

**Theorem 8 (One-parameter exponential family)** *Let  $l_n$  denote the average negative log-likelihood optimized by  $\hat{\beta}_0 = g^{-1}(\hat{\theta}^{\text{MLE}})$  when  $\beta = \mathbf{0}$ . Assume  $\hat{\beta}_0$  is consistent and  $\beta_0$  does not depend on  $n$ ,  $d \in C^3$ ,  $T(Y)$  has finite fourth moment. Under Conditions 1 and 2, PIC is asymptotically pivotal for*

$$(\phi, g) = (\text{id}, \tilde{d}^{-1}) \quad \text{with} \quad \tilde{d}(\theta) = \int^\theta \sqrt{d''(s)} \, ds.$$

A close look at the proof of Theorem 8 shows that the first two moments of  $\Lambda$  are always asymptotically pivotal, but, in particular, Condition 2 on  $B_n$  is needed for the higher moments to be pivotal as well. This condition implies that  $X$  needs to be sufficiently dense.

**Example 1 (Bernoulli)** *In canonical form,  $\log f(y|\theta) = y\theta - \log(1 + e^\theta)$  with  $\theta = \log \frac{\mu}{1-\mu}$  and  $d''(\theta) = \frac{e^\theta}{(1+e^\theta)^2}$ . So  $\tilde{d}(\theta) = 2 \arctan(e^{\theta/2})$  (up to a constant) and*

$$\theta_i = g(\eta_i) = 2 \log \left( \tan \frac{\eta_i + C}{2} \right), \quad \eta_i = \beta_0 + \mathbf{x}_i^T \beta$$

*with  $C$  is an arbitrary centering constant. Correspondingly, the Bernoulli parameters are*

$$\mu_i = \frac{1}{1 + \exp(-2 \log(\tan \frac{\eta_i + C}{2}))} = \sin^2 \left( \frac{\eta_i + C}{2} \right).$$

*Choosing  $C = \pi/2$  gives  $\mu(0) = 1/2$ , leading to  $\mu_i = (\sin(\eta_i) + 1)/2$  for  $\eta_i \in [-\pi/2, \pi/2]$ ,  $i = 1, \dots, n$ .*

The pivotal reparametrization simplifies the variance structure, but it may yield link functions that are monotone only on a restricted interval. For Bernoulli, for example, the parameters need to satisfy linear inequality constraints of the form  $\|\beta_0 + X\beta\|_\infty \leq \pi/2$ . This induces constrained optimization in  $(\beta_0, \beta)$ , which is undesirable for computation. This motivates the second approach.

**Theorem 9 (Weighted score loss)** *Under the same assumptions as Theorem 8, PIC is asymptotically pivotal for  $(\phi, g) = (\text{id}, \text{id})$  when considering the loss function*

$$l_n(\theta, \mathcal{D}) = \frac{1}{n} \sum_{i=1}^n \int^{\theta_i} \frac{d'(s) - T(y_i)}{\sqrt{d''(s)}} \, ds.$$

If one is interested in using another link function  $g \neq \text{id}$ , the proof of Theorem 9 derives the corresponding weighted loss.

**Example 2 (Bernoulli)** *Basic integration leads to the loss  $l_n(\boldsymbol{\theta}, \mathcal{D}) = \frac{1}{n} \sum_{i=1}^n 2y_i e^{-\theta_i/2} + 2(1 - y_i) e^{\theta_i/2}$  with  $\theta_i = \beta_0 + \mathbf{x}_i^T \boldsymbol{\beta}$ , or, with  $\mu_i = 1/(1 + e^{-\theta_i})$ ,*

$$\frac{1}{n} \sum_{i=1}^n 2y_i \sqrt{\frac{1 - \mu_i}{\mu_i}} + 2(1 - y_i) \sqrt{\frac{\mu_i}{1 - \mu_i}}.$$

**Example 3 (Poisson)** *In canonical form,  $\log f(y|\theta) = y\theta - \exp(\theta)$  with  $\theta = \log(\mu)$  and  $d'(\theta) = d''(\theta) = \exp(\theta)$ . The corresponding weighted loss is  $l_n(\boldsymbol{\theta}, \mathcal{D}) = \frac{1}{n} \sum_{i=1}^n 2y_i e^{-\theta_i/2} + 2e^{\theta_i/2}$  with  $\theta_i = \beta_0 + \mathbf{x}_i^T \boldsymbol{\beta}$ , or, with  $\mu_i = \exp(\theta_i)$ ,*

$$\frac{1}{n} \sum_{i=1}^n 2 \frac{y_i}{\sqrt{\mu_i}} + 2\sqrt{\mu_i}.$$

Table 1 summarizes common instances and reports the corresponding gradient expressions  $\nabla$  entering the zero-thresholding statistic  $\Lambda = \|\nabla\|_\infty$ . For the one-parameter exponential family, the link  $g$  and loss are expressed for the natural distribution parameter  $\mu$ . We also list two transformations for the Laplace case and Cox’s survival analysis.

## 2.4 The pivotal detection boundary $\lambda_\alpha^{\text{PDB}}$ in practice

The pivotal detection boundary  $\lambda_\alpha^{\text{PDB}}$  is defined as the  $(1 - \alpha)$ -quantile of the random variable  $\Lambda$  in Proposition 5. By construction for the prescribed pairs  $(\phi, g)$ , the random variable  $\Lambda$  is pivotal for the location–scale family and asymptotically pivotal for the one-parameter exponential family, so its (asymptotic) distribution does not depend on the nuisance parameters  $\boldsymbol{\tau} = (\beta_0, \sigma)$ . Hence, a natural approach to evaluate  $\lambda_\alpha^{\text{PDB}}$  is Monte Carlo simulation. Specifically, one generates  $M$  response vectors  $\mathbf{y}_0^{(m)}$ ,  $m = 1, \dots, M$ , under the null model  $\mathbf{Y}_0 \sim p_\boldsymbol{\tau}$  for any chosen nuisance parameters  $\boldsymbol{\tau}$ , compute  $\lambda^{(m)} = \|\nabla^{(m)}\|_\infty$ , and take the empirical  $(1 - \alpha)$ -quantile of  $\lambda^{(1)}, \dots, \lambda^{(M)}$ . Increasing  $M$  yields an arbitrarily accurate *finite-sample* approximation of  $\lambda_\alpha^{\text{PDB}}$ .

Despite its conceptual appeal and highly parallelizable nature, the Monte Carlo calibration may become computationally demanding in practice. This is especially true in large sample settings or settings where the evaluation of the gradient requires repeated maximum likelihood computations without closed form (e.g., Gumbel). This motivates the following result that bypasses explicit simulations of  $\mathbf{Y}_0$ .

**Proposition 10 (Asymptotic Gaussian calibration)** *Under Conditions 1 and 2, let  $\hat{\Sigma}_X = \frac{1}{n} \sum_{i=1}^n \mathbf{x}_i \mathbf{x}_i^T$  denote the (normalized) Gram matrix. For the models given in Table 1 with their corresponding transformations  $(\phi, g)$  and constant  $c$ , an asymptotic approximation is*

$$F_\Lambda^{-1}(1 - \alpha) \approx q_{1-\alpha} \left( \frac{1}{\sqrt{n}} \left\| \mathcal{N}(0, c \hat{\Sigma}_X) \right\|_\infty \right),$$

where  $q_{1-\alpha}$  denotes the  $(1 - \alpha)$ -quantile.

Law	Loss $l_n$	$g(u)$	Dom( $g$ )	$\phi(v)$	$\nabla$	$c$
<i>Location-scale family</i>						
Gaussian	NLL	$u$	$\mathbb{R}$	$\exp v$	$\sqrt{\frac{2\pi e}{n}} \frac{X^T(\mathbf{y}-\bar{\mathbf{y}}\mathbf{1})}{\ \mathbf{y}-\bar{\mathbf{y}}\mathbf{1}\ _2}$	$2\pi e$
Gaussian	MSE	$u$	$\mathbb{R}$	$\sqrt{v}$	$\frac{X^T(\mathbf{y}-\bar{\mathbf{y}}\mathbf{1})/\sqrt{n}}{\ \mathbf{y}-\bar{\mathbf{y}}\mathbf{1}\ _2}$	1
Gumbel	NLL	$u$	$\mathbb{R}$	$\exp v$	$\frac{e^{1+\bar{\mathbf{z}}}}{n} X^T(e^{\mathbf{z}} - \mathbf{1})^{(*)}$	$e^{2(\gamma+1)}$
Subbotin ( $r > 1$ )	$Mr^{\text{th}}E$	$u$	$\mathbb{R}$	$v^{1/r}$		$\frac{r^{2-2/r}\Gamma(2-1/r)}{\Gamma(1/r)}$
Laplace ( $r = 1$ )	MAE	$u$	$\mathbb{R}$	$v$	$X^T \text{sign}(\mathbf{y} - y_m\mathbf{1})/n^\dagger$	1
<i>One-parameter exponential family</i>						
Bernoulli	NLL	$\frac{1+\sin u}{2}$	$[-\frac{\pi}{2}, \frac{\pi}{2}]$	$v$	$\frac{X^T(\mathbf{y}-\bar{\mathbf{y}}\mathbf{1})/n}{\sqrt{\bar{\mathbf{y}}(1-\bar{\mathbf{y}})}}$	1
Bernoulli	WSL	$\frac{1}{1+e^{-u}}$	$\mathbb{R}$	$v$	$\frac{X^T(\mathbf{y}-\bar{\mathbf{y}}\mathbf{1})/n}{\sqrt{\bar{\mathbf{y}}(1-\bar{\mathbf{y}})}}$	1
Poisson	NLL	$\frac{u^2}{4}$	$\mathbb{R}^+$	$v$	$\frac{X^T(\mathbf{y}-\bar{\mathbf{y}}\mathbf{1})/n}{\sqrt{\bar{\mathbf{y}}}}$	1
Poisson	WSL	$\exp u$	$\mathbb{R}$	$v$	$\frac{X^T(\mathbf{y}-\bar{\mathbf{y}}\mathbf{1})/n}{\sqrt{\bar{\mathbf{y}}}}$	1
Exponential	NLL	$\exp u$	$\mathbb{R}$	$v$	$\frac{X^T(\mathbf{y}-\bar{\mathbf{y}}\mathbf{1})/n}{\bar{\mathbf{y}}}$	1
<i>Survival analysis</i>						
Cox model	NLPL	$u$	$\mathbb{R}$	$\sqrt{v}$	(§)	$\frac{1}{4\log n}$

Table 1: Examples of transformation pairs  $(g, \phi)$  for constructing PIC. The notation 'NLL' is for the negative log-likelihood, 'WSL' is for the weighted score loss, MSE for the mean squared error and MAE for the mean absolute error. For the one-parameter exponential family,  $g$  maps the natural distribution parameter.

(\*)  $\mathbf{z} = (\mathbf{y} - \hat{\mu}\mathbf{1}_n)/\hat{\sigma}$  and  $\bar{\mathbf{z}} = (\bar{\mathbf{y}} - \hat{\mu})/\hat{\sigma}$ , where  $\hat{\mu}$  and  $\hat{\sigma}$  are the MLEs; (†)  $y_m$  is the median (Sardy et al., 2025); (§) 'NLPL' is Cox's negative log-partial likelihood (van Cutsem and Sardy, 2025).

This result is proven for the one-parameter exponential family in Theorem 8 and follows from van de Geer et al. (2025) for the location-scale family.

This *asymptotic calibration* reduces the problem to simulating Gaussian vectors with covariance  $\hat{\Sigma}_X$ , thereby avoiding repeated MLE computations. A further simplification neglects correlations among regressors by replacing  $\hat{\Sigma}_X$  by the identity matrix:

$$q_{1-\alpha} \left( \frac{1}{\sqrt{n}} \|\mathcal{N}(0, I_p)\|_\infty \right) \approx \frac{1}{\sqrt{n}} \Phi^{-1} \left( 1 - \frac{\alpha}{2p} \right) \approx \sqrt{\frac{2}{n} \log \left( \frac{2p}{\alpha} \right)}.$$

This yields a simple closed-form rule for PIC’s pre-set  $\lambda$ , albeit slightly conservative.

## 2.5 Giving BIC a second chance

Section 1.2 showed that the Bayesian Information Criterion (BIC) has a low probability of exact support recovery in moderate to high dimension. To fix BIC, we simply need to derive the zero-thresholding function of the discrete complexity measure (4) for an appropriate  $(\phi, g)$ -transformation such that the corresponding statistic  $\Lambda$  is pivotal. As it turns out, the following theorem states that, with no transformation, BIC is already pivotal so that  $\lambda$  can be selected at the pivotal detection boundary.

**Theorem 11 (Pivotal BIC)** *Consider the discrete measure of complexity  $C$  defined in (4) and let  $l_n(\boldsymbol{\theta}, \sigma; \mathcal{D})$  be twice the negative log-likelihood of the Gaussian law employed by BIC. Then, with the identity transformations  $(g, \phi) = (\text{id}, \text{id})$ , the zero-thresholding function is*

$$\lambda_0(L, \mathcal{D}) = \max_{s=1, \dots, \min(p, n-2)} \frac{1}{s} \log \left( \frac{\text{RSS}_0}{\text{RSS}_s} \right) \tag{9}$$

with  $\text{RSS}_s$  defined in (6), and the resulting IC is finite sample pivotal.

Theorem 11 shows that BIC can be embedded within the PIC framework by calibrating its penalty at the detection edge. In practice, however, computing the BIC’s zero-thresholding function (9) is infeasible in high dimension, as it requires solving an NP-hard optimization problem. This drawback highlights another advantage of using PIC’s continuous penalty. A natural compromise for BIC is to replace best subset selection by a discrete notion of local minimality. For (one step) forward selection, the corresponding zero-thresholding function reduces to  $\lambda_0(L, \mathcal{D}) = \log \left( \frac{\text{RSS}_0}{\text{RSS}_1} \right)$ .

## 3 Simulation studies

### 3.1 Illustration of (non-)pivotal transformations

Figure 1 illustrates the pivotal detection boundary mechanism induced by a suitable pair  $(\phi, g)$  in the canonical Poisson model ( $X = I_n$ ) with unknown background intensity  $\theta_0$ . Since  $X = I_n$ , the multivariate loss decomposes into  $n$  independent univariate losses, and the components of the gradient  $\nabla_{\boldsymbol{\beta}}(\phi \circ l_n \circ g)(\mathbf{0}, \hat{\boldsymbol{\beta}}_0; \mathcal{D})$  provide the information needed to distinguish signals from noise.

The top row shows three simulated datasets ( $n = 500$ ) with background mean  $\mu_0 \in \{36, 4, 144\}$  and sparsity levels  $s \in \{0, 3, 3\}$ , where the nonzero coefficients scale proportionally with  $\mu_0$ . The second row displays the componentwise magnitude  $|\nabla_{\boldsymbol{\beta}}(\phi \circ l_n \circ g)(\mathbf{0}, \hat{\boldsymbol{\beta}}_0; \mathcal{D})|$ ,

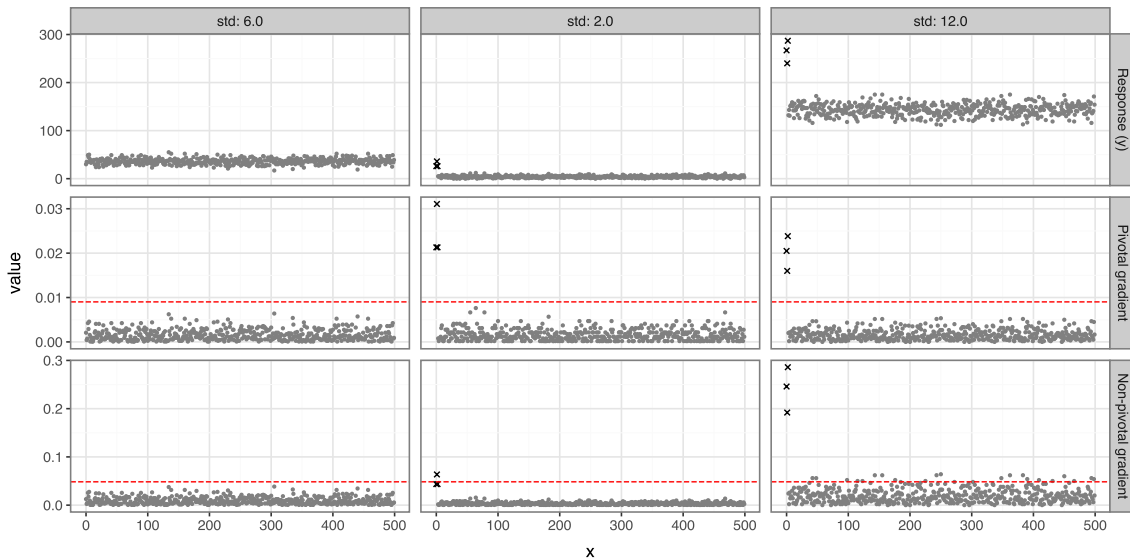


Figure 1: Illustration of the detection boundary induced by PIC's composite loss in the canonical Poisson model ( $X = I_n$ ). Top row: simulated datasets with varying background intensities and sparsity levels  $s \in \{0, 3, 3\}$ . Middle row: component-wise magnitude of the pivotal gradient. Bottom row: corresponding analysis for the non pivotal gradient of the canonical GLM choice.

obtained using PIC's pivotal pair  $(\phi, g) = (\text{id}, \frac{v^2}{4})$  for the average negative log-likelihood  $l_n$ . The red line indicates  $\lambda_\alpha^{\text{PDB}}$ , the  $\alpha$ -upper quantile of  $\Lambda$  with  $\alpha = 0.05$ . By construction, the resulting detection boundary is invariant across the null hypothesis  $H_0$  (left panel) and the alternative scenarios  $H_1$  (middle and right panels) and cleanly separates the signal components from the background noise. Under the null ( $s = 0$ ), the pivotal calibration correctly thresholds all coefficients to zero, while under the alternatives ( $s = 3$ ) it successfully identifies the true signals and suppresses spurious fluctuations.

In contrast, the third row shows the analysis performed with the canonical GLM choice  $(\phi, g) = (\text{id}, \text{exp})$ . Here the detection boundary depends on the data through nuisance parameter estimation and therefore varies across panels. But when these nuisance parameters are poorly estimated (overestimated on bottom middle plot and underestimated on the bottom right plot), the resulting threshold fails to reliably distinguish signals from noise.

### 3.2 Empirical Phase Transition Analysis

We evaluate the performance of the proposed methods through an empirical phase transition analysis in the probability of exact support recovery (PESR) as a function of the sparsity level  $s$ . The study covers three regression settings: Gaussian, logistic, and Gumbel regression. We compare our approaches against three established baselines: BIC, EBIC,

and GLMNet. The first two perform variable selection by minimizing

$$\begin{aligned} \text{BIC}(s) &= -2 \log L_n(\hat{\beta}_0, \hat{\beta}_s) + s \log n, \\ \text{EBIC}_\gamma(s) &= -2 \log L_n(\hat{\beta}_0, \hat{\beta}_s) + s \log n + 2\gamma \log \binom{p}{s}, \end{aligned}$$

where  $L_n$  denotes the likelihood function and  $\gamma = 0.5$ . Both BIC and EBIC are implemented via forward selection. The third baseline uses the `glmnet` package in R to compute the LASSO estimator with the regularization parameter chosen by 10-fold cross-validation minimizing the empirical loss.

For each sparsity level  $s$ , we generate  $m = 200$  independent datasets. The linear predictor is defined as  $\eta_i^{(s)} = \beta_0 + \mathbf{x}_i^\top \boldsymbol{\beta}_s$  for  $i = 1, \dots, n$ , where  $\beta_0 = 0$ ,  $\mathbf{x}_i \in \mathbb{R}^p$  has independent standard Gaussian entries, and  $\boldsymbol{\beta}_s \in \mathbb{R}^p$  contains exactly  $s$  non-zero coefficients, each set to 3. The support of  $\boldsymbol{\beta}_s$  is selected uniformly at random for each dataset. The response variables  $y_i^{(s)}$  are generated conditionally on  $\eta_i^{(s)}$ .

For the Gaussian case,  $y_i^{(s)} = \eta_i^{(s)} + \epsilon_i$  with  $\epsilon_i$  drawn from standard Gaussians. We fix  $p = 100$  and consider  $n \in \{50, 100, 200\}$  in order to explore regimes ranging from high-dimensional ( $n < p$ ) to overdetermined ( $n > p$ ). Both PIC:SCAD and PIC: $\ell_1$  are constructed according to (3), with  $l_n$  the mean squared error loss with the appropriate transformations  $\phi = \sqrt{\cdot}$  and  $g = \text{id}$ , as specified in Table 1. The regularization parameter is selected as  $\lambda_\alpha^{\text{PDB}}$  with  $\alpha = 0.05$ . The PIC:SCAD variant uses the SCAD penalty with parameter  $a = 3.7$  (default value). PIC: $\ell_0$  follows the proposed procedure described in Section 2.5. Figure 2 presents the results. Among the compared procedures, our methods are the only ones that exhibit a sharp phase transition. In particular, the transition between near-perfect recovery and systematic failure is clearly visible, and shifts with increasing  $n$ . Among the baselines, EBIC consistently outperforms BIC, especially in the high-dimensional regime. BIC performs reasonably only when  $n \gg p$ , where the classical asymptotic justification becomes more appropriate. GLMNet performs worst overall in terms of exact support recovery, typically failing to display a clear phase transition and showing substantially lower PESR values across sparsity levels.

In the logistic regression setting, the responses are generated as  $y_i^{(s)} \sim \text{Bernoulli}(\sigma(\eta_i^{(s)}))$  where  $\sigma(t) = 1/(1 + e^{-t})$  denotes the logistic function. In this case, both PIC:SCAD and PIC: $\ell_1$  are implemented using the weighted score loss introduced in Theorem 9, together with the corresponding transformations specified in Table 1. The results for  $p = 100$  and  $n \in \{75, 150, 300\}$  are displayed in Figure 3. The behavior mirrors that of the Gaussian setting: our methods display a clear phase transition, whereas the baselines show a more gradual degradation in performance. Compared to the Gaussian setting, the logistic case highlights the increased difficulty of binary classification for exact support recovery.

For the Gumbel regression setting,  $y_i^{(s)} = \eta_i^{(s)} + \epsilon_i$  with  $\epsilon_i$  drawn from Gumbel(0, 2). Figure 3 presents the corresponding phase transition results. Here, baseline comparisons are not included, as neither `glmnet` nor `statsmodels` (used for the forward-selection-based competitors) provides direct support for this model. Consequently, the analysis focuses on the proposed PIC-based methods, which again exhibit a clear phase transition.

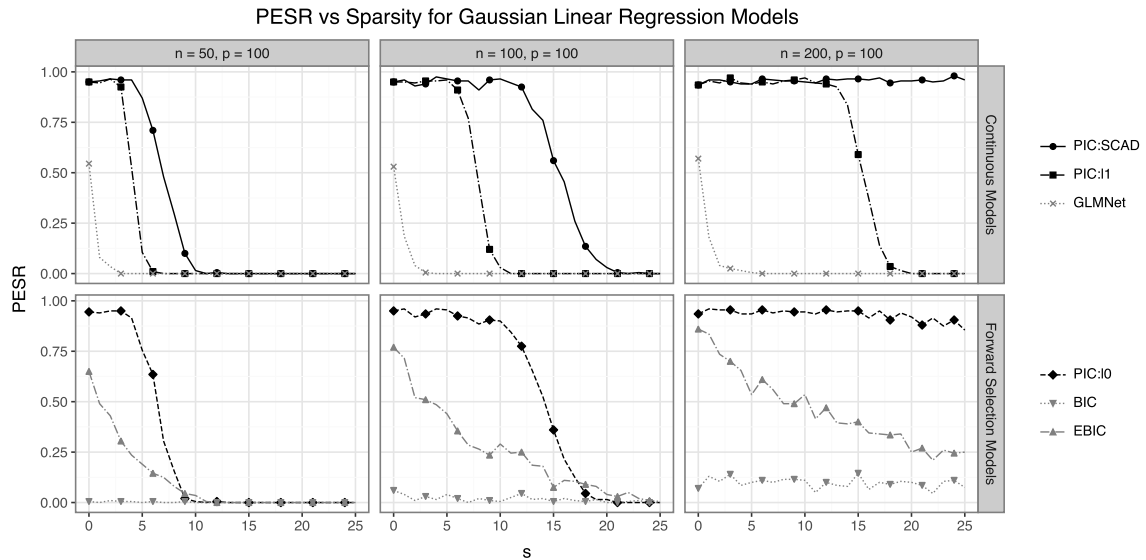


Figure 2: Phase transition behaviour in exact support recovery for the Gaussian linear model. Top row: results for the continuous complexity measure  $C$ . Bottom row: result for the discrete  $C$  employing forward selection.

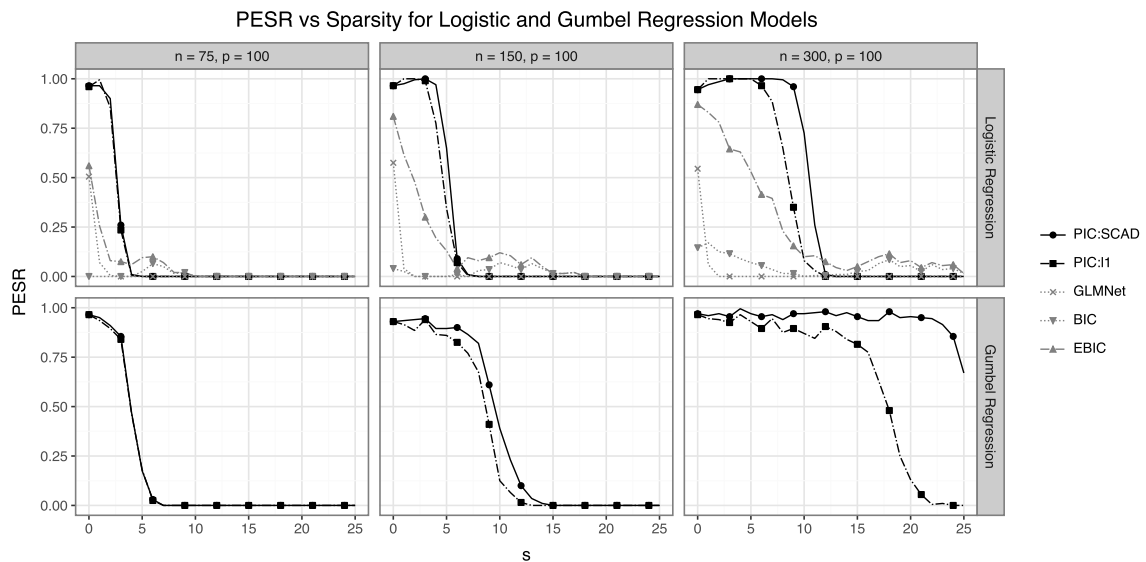


Figure 3: Phase transition behaviour in exact support recovery for the logistic (top) and Gumbel (bottom) regression model.

### 3.3 Real data experiments

We now complement the synthetic phase transition analysis with an empirical study on real-world datasets, focusing on both variable selection behavior and predictive performance. In particular, we consider six datasets: three corresponding to Gaussian regression tasks and three corresponding to binary classification problems. For each dataset, categorical variables are encoded using dummy variables when applicable, and missing values are handled via simple imputation using either the mean (for numerical variables) or the most frequent category (for categorical variables). All covariates are standardized before training. Table 2 summarizes the main characteristics of each dataset after preprocessing.

Dataset	Source	$n$	$p$
<b>Regression datasets</b>			
Prostate Cancer	Kaggle	97	8
Communities & Crime	UCI	1994	100
Riboflavin	R: hdi	71	4088
<b>Binary classification datasets</b>			
Breast Cancer	scikit-learn	569	30
Ionosphere	UCI	351	33
Sonar	UCI	208	60

Table 2: Considered datasets with some key characteristics.

For each dataset, we perform 100 independent random train-test splits, where the test set represents 30% of the total observations and the remaining 70% is used for training. All model fitting and variable selection procedures are carried out exclusively on the training data, after which predictive performance is evaluated on the test set. Performance metrics are chosen according to the task: mean squared error is used for regression tasks, whereas classification accuracy is used for binary classification. Following variable selection, all methods are refitted without regularization on the selected features prior to evaluation.

Table 3 summarizes the results. Overall, the conclusions are consistent with those observed in the previous section. The cross-validated GLMNet approach achieves strong predictive performance but tends to retain a relatively large number of features, resulting in less parsimonious models. In contrast, the information criterion-based approaches, particularly EBIC, consistently select substantially smaller subsets of variables while maintaining competitive predictive accuracy. However, for similar levels of predictive accuracy, the PIC procedures achieve greater parsimony by selecting fewer variables. According to Occam’s razor this makes the PIC approaches particularly appealing in practice.

## 4 Conclusions and future work

BIC has been known to underpenalize complexity, causing false detections in many data analyses. Attempts to alleviate this problem have been to increase BIC’s penalty (e.g., EBIC and GIC) or to modify cross-validation with the one standard error rule (Breiman

Dataset	PIC:SCAD	PIC: $\ell_1$	PIC: $\ell_0$	GLMNet	BIC	EBIC
<b>Regression</b>						
Prostate Cancer	0.60 $2.7 \pm 0.1$	0.58 $3.2 \pm 0.1$	0.64 $2.2 \pm 0.1$	0.59 $5.8 \pm 0.2$	0.59 $3.0 \pm 0.1$	0.60 $2.9 \pm 0.1$
Communities & Crime	0.02 $12.5 \pm 0.2$	0.02 $12.5 \pm 0.2$	0.02 $9.0 \pm 0.2$	0.02 $58.3 \pm 2.2$	0.02 $11.6 \pm 0.3$	0.02 $10.7 \pm 0.2$
Riboflavin	0.35 $6.1 \pm 0.2$	0.36 $6.1 \pm 0.2$	0.53 $2.4 \pm 0.1$	0.48 $35.5 \pm 1.4$	0.67 $48.8 \pm 0.1$	0.46 $8.7 \pm 1.2$
<b>Classification</b>						
Breast Cancer	0.96 $3.5 \pm 0.1$	0.96 $4.2 \pm 0.1$	–	0.96 $13.0 \pm 0.3$	0.96 $5.6 \pm 0.3$	0.96 $5.0 \pm 0.2$
Ionosphere	0.87 $4.3 \pm 0.1$	0.87 $4.6 \pm 0.1$	–	0.88 $16.6 \pm 0.4$	0.87 $11.3 \pm 0.5$	0.87 $8.9 \pm 0.3$
Sonar	0.71 $3.0 \pm 0.2$	0.71 $3.8 \pm 0.2$	–	0.73 $20.1 \pm 0.6$	0.73 $13.8 \pm 0.6$	0.72 $7.1 \pm 0.5$

Table 3: Comparison of PIC-based methods with GLMNet, BIC, and EBIC on standard regression and classification benchmarks. The first line in each entry reports the mean predictive performance. For regression tasks, performance is measured by predictive error (lower is better), whereas for classification tasks performance is measured by accuracy (higher is better). The second line in each entry reports the average model size (mean  $\pm$  standard deviation) over repeated data splits.

et al., 1984). These methods seem ad hoc and have not been designed to induce a phase transition. In empirical studies, these methods tend to select too many covariates.

The proposed method defines a new general framework to balance generalization and complexity in a way that mimics the phase transition achieved by compressed sensing. The probabilistic selection of  $\lambda$  is calibrated to control the false discovery rate under the null model. PIC generalizes square-root LASSO to the location-scale and one-parameter exponential families, and can be naturally extended further beyond linear models and beyond regression or classification tasks; van Cutsem and Sardy (2025) apply PIC to survival analysis. The pivotality property of the gradient could also be employed further in gradient-based regularization.

### Appendix A. Proof of Theorem 4

Let  $f(\boldsymbol{\beta}, \boldsymbol{\tau}) = L(\boldsymbol{\beta}, \boldsymbol{\tau}) + \lambda C(\boldsymbol{\beta})$  with  $C \in \mathcal{C}_{\ell_1}$ . Denote  $\boldsymbol{\zeta} = (\boldsymbol{\beta}, \boldsymbol{\tau})$ ,  $\boldsymbol{\zeta}^0 = (\mathbf{0}, \hat{\boldsymbol{\tau}})$ , where  $\hat{\boldsymbol{\tau}}$  minimizes  $L$  at  $\boldsymbol{\beta} = \mathbf{0}$ . Let  $\boldsymbol{\zeta}^\epsilon = \boldsymbol{\zeta}^0 + \epsilon \mathbf{h}$  with  $\mathbf{h} = (d_\beta, d_\tau)$ . A second-order Taylor expansion of  $L$  around  $\boldsymbol{\zeta}^0$ , combined with the first-order optimality conditions in  $\boldsymbol{\tau}$ , yields

$$L(\boldsymbol{\zeta}^\epsilon) = L(\boldsymbol{\zeta}^0) + \epsilon d_\beta^\top \nabla_\beta L(\boldsymbol{\zeta}^0) + \frac{\epsilon^2}{2} \mathbf{h}^\top H_\zeta(\boldsymbol{\zeta}^0) \mathbf{h} + o(\epsilon^2).$$

Since  $C \in \mathcal{C}_l$ ,

$$f(\boldsymbol{\zeta}^\epsilon) - f(\boldsymbol{\zeta}^0) = \epsilon d_\beta^\top \nabla_\beta L(\boldsymbol{\zeta}^0) + \frac{\epsilon^2}{2} \mathbf{h}^\top H_\zeta(\boldsymbol{\zeta}^0) \mathbf{h} + \lambda |\epsilon| \|d_\beta\|_1 + o(\epsilon^2).$$

By Hölder's inequality,  $|d_\beta^\top \nabla_\beta L(\boldsymbol{\zeta}^0)| \leq \|\nabla_\beta L(\boldsymbol{\zeta}^0)\|_\infty \cdot \|d_\beta\|_1$ , which implies

$$f(\boldsymbol{\zeta}^\epsilon) - f(\boldsymbol{\zeta}^0) \geq |\epsilon| (\lambda - \|\nabla_\beta L(\boldsymbol{\zeta}^0)\|_\infty) \|d_\beta\|_1 + \frac{\epsilon^2}{2} \mathbf{h}^\top H_\zeta(\boldsymbol{\zeta}^0) \mathbf{h} + o(\epsilon^2).$$

Writing  $\mathbf{h}^\top H_\zeta(\boldsymbol{\zeta}^0) \mathbf{h} = d_\beta^\top H_{\beta\beta} d_\beta + 2d_\beta^\top H_{\beta\tau} d_\tau + d_\tau^\top H_{\tau\tau} d_\tau$ , we distinguish directions with  $d_\beta = \mathbf{0}$ , for which positivity follows from  $H_{\tau\tau}(\boldsymbol{\zeta}^0) \succ 0$ , and directions with  $d_\beta \neq \mathbf{0}$ , where the linear penalty term dominates all quadratic contributions for sufficiently small  $\epsilon$ . Hence  $\boldsymbol{\zeta}^0$  is a local minimizer of  $f$  if and only if

$$\lambda > \|\nabla_\beta L(\boldsymbol{\zeta}^0)\|_\infty,$$

yielding the stated zero-thresholding function.

### Appendix B. Proof of Theorem 7

For the location-scale family, the negative log-likelihood is  $l_n(\theta, \sigma; \mathcal{D}) = \log \sigma - 1/n \sum_{i=1}^n \log f((y_i - \theta)/\sigma)$ . So with  $\phi = \exp$ , the zero-thresholding function is

$$\begin{aligned} \lambda_0(\exp(l_n), \mathcal{D}) &= \exp\left(\log \hat{\sigma}^{\text{MLE}} - \frac{1}{n} \sum_{i=1}^n \log f\left(\frac{y_i - \hat{\theta}^{\text{MLE}}}{\hat{\sigma}^{\text{MLE}}}\right)\right) \\ &\quad \cdot \left\| X^\top \frac{1}{n \hat{\sigma}^{\text{MLE}}} \sum_{i=1}^n \frac{f'((y_i - \hat{\theta}^{\text{MLE}})/\hat{\sigma}^{\text{MLE}})}{f((y_i - \hat{\theta}^{\text{MLE}})/\hat{\sigma}^{\text{MLE}})} \right\|_\infty \\ &= \frac{1}{n} \exp\left(-\frac{1}{n} \sum_{i=1}^n \log f\left(\frac{y_i - \hat{\theta}^{\text{MLE}}}{\hat{\sigma}^{\text{MLE}}}\right)\right) \cdot \left\| X^\top \sum_{i=1}^n \frac{f'((y_i - \hat{\theta}^{\text{MLE}})/\hat{\sigma}^{\text{MLE}})}{f((y_i - \hat{\theta}^{\text{MLE}})/\hat{\sigma}^{\text{MLE}})} \right\|_\infty. \end{aligned}$$

Suppose  $\mathcal{D}' = (X, \mathbf{y}')$  with  $\mathbf{y}' = a\mathbf{y} + b$  with  $a > 0$ , then, by definition of the location scale family,  $\mathbf{y}'$  is a sample from the same law as  $\mathbf{y}$  but with parameters  $(\theta', \sigma')$ . Moreover, since an affine transform is monotone, we have that  $\hat{\theta}'^{\text{MLE}} = a\hat{\theta}^{\text{MLE}} + b$  and  $\hat{\sigma}'^{\text{MLE}} = a\hat{\sigma}^{\text{MLE}}$ . So  $\lambda_0(\exp \circ l_n, \mathcal{D}') = \lambda_0(\exp \circ l_n, \mathcal{D})$ , proving that PIC is pivotal for the location-scale family.

### Appendix C. Proof of Theorem 8 and 9

Assuming a one-parameter exponential family in canonical form  $\log f(y_i | \theta_i) = \theta_i T(y_i) - d(\theta_i) + b(y_i)$ , and a link  $\theta_i = g(\eta_i)$  for  $\eta_i = \beta_0 + \mathbf{x}_i^T \boldsymbol{\beta}$  leads to the negative log-likelihood

$$l_n(\boldsymbol{\theta}, \mathcal{D}) = \frac{1}{n} \sum_{i=1}^n d'(\theta_i) - T(y_i).$$

To create pivotality, we rather consider a general class of loss functions of the form

$$l_n(\boldsymbol{\theta}, \mathcal{D}) = \frac{1}{n} \sum_{i=1}^n A(\theta_i) - w(\theta_i) T(y_i),$$

where  $w$  is a differentiable function. Imposing  $A'(\theta) = d'(\theta) w'(\theta)$  ensures Fisher consistency. Note that choosing  $w(\theta) = \theta$  recovers the negative log-likelihood. The considered loss allows for a weighted gradient

$$\mathcal{H} := \{h_{\beta_0}(y_i, \mathbf{x}_i) = (T(y_i) - d'(g(\beta_0))) w'(g(\beta_0)) g'(\beta_0) \mathbf{x}_i, \beta_0 \in \mathcal{C}\},$$

where  $h_{\beta_0}(y_i, \mathbf{x}_i)$  denotes the one-sample gradient with respect to  $\boldsymbol{\beta}$  evaluated at  $\boldsymbol{\beta} = \mathbf{0}$ , and  $\mathcal{C}$  is a compact set. The zero-thresholding function (8) of  $l_n$  is  $\|\frac{1}{n} \sum_{i=1}^n h_{\hat{\beta}_0}(y_i, \mathbf{x}_i)\|_\infty = \|P_n h_{\hat{\beta}_0}\|_\infty$ . Thanks to the centering assumption  $\sum_i \mathbf{x}_i = \mathbf{0}$ ,

$$P_n h_{\hat{\beta}_0} = \frac{1}{n} \sum_{i=1}^n h_{\hat{\beta}_0}(y_i, \mathbf{x}_i) = \frac{1}{n} \sum_{i=1}^n (T(y_i) - d'(g(t))) w'(g(\hat{\beta}_0)) g'(\hat{\beta}_0) \mathbf{x}_i,$$

for all  $t$ , in particular for the true parameter value  $t = \beta_0$ . Therefore

$$\sqrt{n} (P_n h_{\hat{\beta}_0} - P_n h_{\beta_0}) = \sqrt{n} (w'(g(\hat{\beta}_0)) g'(\hat{\beta}_0) - w'(g(\beta_0)) g'(\beta_0)) \cdot \frac{1}{n} \sum_{i=1}^n [T(y_i) - d'(g(\beta_0))] \mathbf{x}_i.$$

Assuming the map  $t \mapsto w(g(t))$  is twice differentiable at  $\beta_0$ , by consistency and the Delta method, the first term is of order  $O_{\mathbb{P}}(1)$ . Moreover, the second term is of the form  $\frac{1}{n} X^T \boldsymbol{\epsilon}$ , where  $\boldsymbol{\epsilon}_i = T(y_i) - d'(g(\beta_0))$  has mean zero and is sub-exponential. Using Hoeffding and union bounds, the second term is of order  $o_{\mathbb{P}}(1)$ . Hence,

$$\left\| \sqrt{n} (P_n h_{\hat{\beta}_0} - P_n h_{\beta_0}) \right\|_\infty = O_{\mathbb{P}}(1) \cdot o_{\mathbb{P}}(1) = o_{\mathbb{P}}(1).$$

So

$$\|\sqrt{n} P_n h_{\hat{\beta}_0}\|_\infty = \|\sqrt{n} P_n h_{\beta_0}\|_\infty + o_{\mathbb{P}}(1).$$

Define  $\mathbf{v}_i = h_{\beta_0}(y_i, \mathbf{x}_i) = (T(y_i) - d'(g(\beta_0))) w'(g(\beta_0)) g'(\beta_0) \mathbf{x}_i = \xi_i \mathbf{x}_i$ , so that  $\|\sqrt{n} P_n h_{\beta_0}\|_\infty = \|\frac{1}{\sqrt{n}} \sum_i \mathbf{v}_i\|_\infty$ . Note that  $\mathbf{v}_i$  are independent vectors and  $v_{ij} = x_{ij} \xi_i$  with  $\mathbb{E}[\xi_i] = 0$  and  $\mathbb{E}[\xi_i^2] = (w'(g(\beta_0)) g'(\beta_0))^2 d''(g(\beta_0))$ . Hence, imposing

$$w'(g(t)) g'(t) = \frac{1}{\sqrt{d''(g(t))}},$$

implies a covariance free of the nuisance parameter. Choosing  $w(\theta) = \theta$  determines the pivotal link  $g$  of Theorem 8, whereas fixing the canonical link  $\theta = g(\eta) = \eta$  leads to the loss of Theorem 9.

Further assuming  $\mathbb{E}[\xi_i^4] < \infty$ , Chernozhukov et al. (2013) showed that, under the assumptions of the theorem,

$$\sup_{t \in \mathbb{R}} \left| \mathbb{P} \left( \|\sqrt{n}P_n h_{\beta_0}\|_\infty \leq t \right) - \mathbb{P} \left( \left\| \frac{1}{\sqrt{n}} \sum_{i=1}^n \mathbf{z}_i \right\|_\infty \leq t \right) \right| \rightarrow 0,$$

where  $\mathbf{z}_1, \dots, \mathbf{z}_n$  are independent centered Gaussian random vectors in  $\mathbb{R}^p$  such that each  $\mathbf{z}_i$  and  $\mathbf{t}_i$  share the same covariance matrix. Consequently, for any fixed  $\alpha \in (0, 1)$ , the  $(1 - \alpha)$ -quantile of  $\|\sqrt{n}P_n h_{\beta_0}\|_\infty$  can be consistently approximated by the  $(1 - \alpha)$ -quantile of  $\|N(0, \Sigma_X)\|_\infty$  with  $\Sigma_X = \frac{1}{n} \sum_{i=1}^n \mathbf{x}_i \mathbf{x}_i^\top$ .

## Appendix D. Proof of Theorem 11

Twice the negative log-likelihood combined with the proposed transformations yields

$$L(\boldsymbol{\beta}, \beta_0, \sigma; \mathcal{D}) = \frac{1}{\sigma^2} \frac{\|\mathbf{y} - \beta_0 \mathbf{1}_n - X\boldsymbol{\beta}\|_2^2}{n} + \log(2\pi\sigma^2).$$

Let  $\text{RSS}_s$  be the best size  $s$  residuals some of squares defined in (6). For fixed  $s$ , we have that  $(\hat{\sigma}^{\text{MLE}})^2 = \text{RSS}_s/n$ , so the profile information criterion is  $\text{IC} = 1 + \log(2\pi\text{RSS}_s/n) + \lambda s$ . To ensure  $s = 0$  is a minimizer of the IC,  $\lambda$  must be large enough so that

$$1 + \log(2\pi\text{RSS}_0/n) \leq 1 + \log(2\pi\text{RSS}_s/n) + \lambda s, \quad \text{for all } s \geq 1.$$

Therefore the zero-thresholding function is that given in (9). So the statistic  $\Lambda = \lambda_0(L, (X, \mathbf{Y}_0))$  is pivotal with respect to  $(\beta_0, \sigma)$  since  $\text{RSS}_s/\sigma^2$  is pivotal for all  $s$ .

## References

- H. Akaike. Information theory and an extension of the maximum likelihood principle. In *Selected Papers of Hirotugu Akaike*, pages 199–213. Springer, 1998.
- M. S. Bartlett. The Use of Transformations. *Biometrics*, 3(1):39–52, 1947.
- A. Belloni, V. Chernozhukov, and L. Wang. Square-root lasso: pivotal recovery of sparse signals via conic programming. *Biometrika*, 98(4):791–806, 2011.
- L. Breiman, J. Friedman, R. Olshen, and C. Stone. *Classification and Regression Trees*. Routledge, Boca Raton, 1984.
- E. Candès and J. Romberg. Sparsity and incoherence in compressive sampling. *Inverse Problems*, 23(3):969–985, 2007.
- J. Chen and Z. Chen. Extended Bayesian information criteria for model selection with large model spaces. *Biometrika*, 95(3):759–771, 2008.

- S. S. Chen, D. L. Donoho, and M. A. Saunders. Atomic decomposition by basis pursuit. *SIAM Journal on Scientific Computing*, 20(1):33–61, 1999.
- V. Chernozhukov, D. Chetverikov, and K. Kato. Gaussian approximations and multiplier bootstrap for maxima of sums of high-dimensional random vectors. *The Annals of Statistics*, 41(6), December 2013.
- D. Donoho and J. Jin. Higher criticism for detection sparse heterogeneous mixtures. *Annals of Statistics*, 32:962–994, 2004.
- D. L. Donoho. Compressed sensing. *IEEE Transactions on Information Theory*, 52:1289–1306, 2006.
- D. L. Donoho and I. M. Johnstone. Ideal spatial adaptation by wavelet shrinkage. *Biometrika*, 81(3):425–455, 1994.
- D. L. Donoho, I. M. Johnstone, G. Kerkyacharian, and D. Picard. Wavelet shrinkage: asymptopia? *Journal of the Royal Statistical Society: Series B*, 57(2):301–369, 1995.
- J. Fan and R. Li. Variable selection via nonconcave penalized likelihood and its oracle properties. *Journal of the American Statistical Association*, 96(456):1348–1360, 2001.
- J. Fan, S. Guo, and N. Hao. Variance estimation using refitted cross-validation in ultrahigh dimensional regression. *Journal of the Royal Statistical Society: Series B*, 74(1):37–65, 2012.
- Y. Fan and C. Y. Tang. Tuning parameter selection in high dimensional penalized likelihood. *Journal of the Royal Statistical Society: Series B*, 75(3):531–552, 2013.
- C. Giacobino, S. Sardy, J. Diaz-Rodriguez, and N. Hengartner. Quantile universal threshold. *Electron. J. Statist.*, 11(2):4701–4722, 2017.
- Y. I. Ingster. Some problems of hypothesis testing leading to infinitely divisible distribution. *Mathematical Methods of Statistics*, 6:47–69, 1997.
- Y. I. Ingster, A. B. Tsybakov, and N. Verzelen. Detection boundary in sparse regression. *Electronic Journal of Statistics*, 4:1476–1526, 2010.
- K. Ito and K. Kunisch. A variational approach to sparsity optimization based on Lagrange multiplier theory. *Inverse Problems*, 30(1), 2014.
- W. James and C. Stein. Estimation with quadratic loss. In *Proceedings of the Fourth Berkeley Symposium on Mathematical Statistics and Probability, Volume 1: Contributions to the Theory of Statistics*, pages 361–379, Berkeley, California, 1961. University of California Press.
- J. A. Nelder and R. W. M. Wedderburn. Generalized linear models. *Journal of the Royal Statistical Society: Series A*, 135(3):370–384, 1972.
- S. Sardy, I. Mizera, Xiaoyu Ma, and H. Gaible. The  $\infty$ -s test via regression quantile affine LASSO. *ArXiv*, arXiv:2409.04256, 2025.

- G. Schwarz. Estimating the dimension of a model. *The Annals of Statistics*, 6(2):461–464, 1978.
- W. Su, M. Bogdan, and E. Candes. False discoveries occur early on the lasso path. *The Annals of Statistics*, 45:2133–2150, 11 2015.
- R. Tibshirani. Regression shrinkage and selection via the lasso. *Journal of the Royal Statistical Society, Series B*, 58(1):267–288, 1996.
- M. van Cutsem and S. Sardy. Square root cox’s survival analysis by the fittest linear and neural networks model. *ArXiv*, arXiv:2510.19374, 2025.
- S. van de Geer, S. Sardy, and M. van Cutsem. A pivotal transform for the high-dimensional location-scale model. *ArXiv*, abs/2109.06098, 2025.
- C.-H. Zhang. Nearly unbiased variable selection under minimax concave penalty. *The Annals of Statistics*, 38(2), 2010.
- H. Zou and T. Hastie. Regularization and variable selection via the elastic net. *Journal of the Royal Statistical Society: Series B*, 67(2):301–320, 2005.